



HAL
open science

MRI-visible polymer based on poly(methyl methacrylate) for imaging applications

Mira Younis, Vincent Darcos, Cédric Paniagua, Pauline Ronjat, Laurent Lemaire, Benjamin Nottelet, Xavier Garric, Youssef Bakkour, John Hanna El Nakat, Jean Coudane

► **To cite this version:**

Mira Younis, Vincent Darcos, Cédric Paniagua, Pauline Ronjat, Laurent Lemaire, et al.. MRI-visible polymer based on poly(methyl methacrylate) for imaging applications. RSC Advances, 2016, 6 (7), pp.5754-5760. 10.1039/C5RA23646K . hal-01388778

HAL Id: hal-01388778

<https://hal.science/hal-01388778>

Submitted on 24 Jan 2024

HAL is a multi-disciplinary open access archive for the deposit and dissemination of scientific research documents, whether they are published or not. The documents may come from teaching and research institutions in France or abroad, or from public or private research centers.

L'archive ouverte pluridisciplinaire **HAL**, est destinée au dépôt et à la diffusion de documents scientifiques de niveau recherche, publiés ou non, émanant des établissements d'enseignement et de recherche français ou étrangers, des laboratoires publics ou privés.



Distributed under a Creative Commons Attribution - NonCommercial 4.0 International License

MRI-visible polymer based on poly(methyl methacrylate) for imaging applications†

Mira Younis,^{ab} Vincent Darcos,^{*a} Cédric Paniagua,^a Pauline Ronjat,^a Laurent Lemaire,^c Benjamin Nottelet,^a Xavier Garric,^a Youssef Bakkour,^d John Hanna El Nakat^b and Jean Coudane^a

Macromolecular contrast agents are very attractive to afford efficient magnetic resonance imaging (MRI) visualization of implantable medical devices. In this work, we report on the grafting of a Gd-based DTPA contrast agent onto a poly(methyl methacrylate) derivative backbone by combining free radical polymerization and copper-catalyzed azide-alkyne cycloaddition (CuAAC). Using free radical polymerization, poly(methyl methacrylate-co-propargyl methacrylate) copolymers were prepared with a control of the ratio in propargyl methacrylate monomer units. The synthesis of a new azido mono-functionalized DTPA ligand was also reported and characterized by ¹H NMR and mass spectroscopy. After complexation with gadolinium, this ligand has been grafted on the polymer backbone by click chemistry reaction. The obtained macromolecular contrast agent was then coated on a polypropylene mesh using the airbrushing technique and the mesh was assessed for MRI visualization at 7 teslas. The polymeric contrast agent was also tested for cytocompatibility and stability to assess its suitability for biomedical applications.

1. Introduction

Magnetic resonance imaging (MRI) has become one of the most popular imaging techniques in the last few decades, with nearly 60 million MRI scans performed yearly around the world.¹ This technique's popularity and routine use by clinicians for diagnosis arises from the fact that it is a non-invasive imaging technique with high spatial resolution.² In order to enhance the signal and thus improve the diagnosis accuracy, various MRI contrast agents (CAs) have been developed. CAs containing paramagnetic ions such as gadolinium (Gd) are currently the most employed owing to the ion's unique magnetic properties^{3,4} and high coordination number.⁵ However, free gadolinium (Gd³⁺) ion is highly toxic. In order to reduce its toxicity, Gd^{III} chelates have been developed.³ Among these Gd^{III} complexes, hydrophilic and low molecular weight complexes such as

Magnevist®, Dotarem®, Omniscan® have been extensively used for clinical uses in the last decades. However, large amount of those low molar masses Gd chelates must be injected as they are rapidly cleared from the body⁶ thus allowing MRI visualization for only short periods of time. To circumvent this clearance shortcoming and also to significantly increase the relaxivity properties as relaxivity enhancement time,⁷ CAs have been linked to macromolecular structures such as polymer,⁸ dendrimer,⁹ carbon nanotube,¹⁰ fullerenes.¹¹ As a consequence, new functional Gd-based CAs were recently prepared to improve the ligation between the macromolecular structure and the CA.

The development of such new functional Gd-based CA that can be grafted on polymeric structures opens up a new era in MR imaging. Indeed, polymeric based implants as used in gynecology or hernia repair are not visible using conventional MR imaging examination^{12,13} even though the presence of collagen coating on some of them allow a transitional visualization of the implant.¹⁴

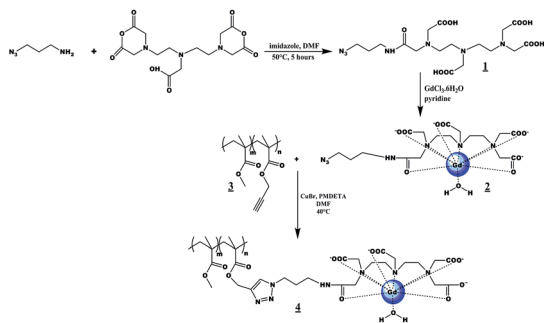
However, a long term visualization of the prosthesis is required to obtain information concerning their post-operation fate and fixation inside the body.^{15,16} Polymeric gadolinium macromolecular contrast agents are one of the very promising contrast agents for long term visualization^{7,17} even if there are not so many examples concerning the use of hydrophobic polymers. Among the first examples of the use of hydrophobic polymers are MRI-visible PCL and MRI-visible PMMA obtained by post-polymerization modification.^{18,19} However, there are some disadvantages concerning the synthesis of these

^aInstitut des Biomolécules Max Mousseron (IBMM), UMR 5247, CNRS, Université Montpellier, ENSCM, Bâtiment I, Faculté de Pharmacie, 15 avenue Charles Flahault, BP14491, 34093 Montpellier cedex 5, France. E-mail: vincent.darcos@univ-montp1.fr

^bDepartment of Chemistry, Faculty of Sciences, University of Balamand, Al Kurah, P.O. Box 100, Lebanon

^cMicro et Nanomédecines Biomimétiques-MINT, INSERM UMR-S1066, Université Angers, 4 rue Larrey, 49933 Angers Cedex 9, France

^dLaboratory of Applied Chemistry, Faculty of Science III, Lebanese University, P.O.Box 826, Tripoli, Lebanon



Scheme 1 Synthetic pathway for the preparation of PMMA MRI contrast agent 4.

polymeric contrast agents, such as lack of control over the substitution degree of the polymer and the necessity to use several protection/deprotection steps on the DTPA ligand before the complexation with gadolinium. In order to control the substitution degree of CA, in a second approach the Huisgen click reaction had been used in the synthesis of MRI poly(ϵ -caprolactone).²⁰

In this paper, we aim at designing and characterizing Gd³⁺-functionalized poly(methyl methacrylate) using copper catalyzed [3 + 2] cycloaddition (Scheme 1). The synthesis of new azide mono-functionalized DTPA and its corresponding gadolinium(III) complex is first reported. Then, the click reaction of a gadolinium DTPA complex onto an alkyne-functionalized poly(methyl methacrylate) is described. The obtained macromolecular contrast agent is then coated on a commercial polypropylene mesh using the airbrushing technique.²¹ The effect of the amount of gadolinium present in the contrast agent on the MRI signal will be assessed, in addition to stability and cytocompatibility studies.

2. Experimental section

2.1. Chemicals and materials

Dimethylformamide (DMF, Aldrich) and toluene (Aldrich) were dried over calcium hydride overnight and distilled under reduced pressure. Pyridine (Aldrich) was dried over KOH and distilled. Tetrahydrofuran (THF, Aldrich) was dried by refluxing over a benzophenone–sodium mixture until a deep blue colour appeared and distilled. Methyl methacrylate (MMA, Aldrich) was purified through a basic aluminum oxide column in order to remove the inhibitor. AIBN was recrystallized in ethanol. All other materials were obtained from Aldrich and were used without any further purification.

2.2. Characterization

2.2.1 NMR spectroscopy. AMX300 Bruker spectrophotometer operating at 300 MHz was used to record the NMR spectra. AMX400 Bruker spectrophotometer was used to obtain the ¹H and ¹³C spectra of the azido functionalized DTPA ligand. Deuterated chloroform and water were used as solvent, and chemical shifts were expressed in ppm with respect to tetramethylsilane (TMS).

2.2.2 FT-IR. FT-IR spectra were obtained on a Perkin Elmer spectrum 100 FT-IR spectrophotometer with an attenuated total reflectance (ATR) method.

2.2.3 LC-MS and MALDI analyses. A Q-TOF (Waters) spectrometer with an electrospray interface was used to obtain LC-MS spectra. An Ultra-FlexIII spectrometer (Bruker) with dithranol as matrix was used to obtain MALDI-TOF spectra. All solvents were HPLC grade.

2.2.4 Preparative HPLC. HPLC separation was performed at SYNBO3, Montpellier on HPLC (Waters) with HD-C18 column using HPLC acetonitrile in 0.1% trifluoroacetic acid as eluent.

2.2.5 Size exclusion chromatography. Size exclusion chromatography (SEC) was performed at room temperature using a Viscotek GPCmax system equipped with a Viscotek guard column (10 × 4.6 mm) and two Viscotek columns LT 5000L mixed medium (300 × 7.8 mm), with a Viscotek VE 3580 refractometric detector, and a Viscotek VE 3210 UV/Vis detector. Calibration was established with polystyrene standards from Polymer Laboratories. THF was used as solvent with a flow rate of 1 mL min⁻¹.

2.2.6 ICP-MS analyses. Quantification of Gd³⁺ and Cu⁺ was performed on an Element XR sector field ICP-MS (inductively coupled plasma) with an indium enriched ultrapure solution as an internal standard. The analyses were performed in the GeoSciences laboratory at the University of Montpellier.

2.3. Synthesis

2.3.1 Synthesis of 3-azido-1-propylamine. 3-Azido-1-propylamine was synthesized according to a known procedure.²² 3-Chloropropylamine hydrochloride (4 g, 30.8 mmol), sodium azide (6 g, 92.3 mmol), and water (30 mL) were added in the round bottom flask. The mixture solution was heated overnight at 80 °C. After cooling in an ice bath, KOH (4 g) and diethyl ether (50 mL) were added. After separation of the organic phase, the aqueous phase was further extracted with diethyl ether (3 × 50 mL). The organic phase was then dried over magnesium sulfate and evaporated under reduced pressure. Purification of the crude product by distillation yielded 2.46 g of the pure product as colorless oil with a yield of 80%. ¹H NMR (300 MHz, CDCl₃): δ (ppm) = 3.3 (t, 2H, CH₂N₃); 2.8 (t, 2H, CH₂NH₂), 1.6 (m, 2H, CH₂CH₂CH₂), 1.4 (s, NH₂). FT-IR (ATR, cm⁻¹): 2100 (N₃).

2.3.2 Synthesis of azido-functionalized DTPA (mono N₃-DTPA). DTPA bis-anhydride (1.9 g, 5.3 mmol, 1 equiv.) and imidazole (3.04 g, 44.2 mmol) were solubilized in DMF at 80 °C. The mixture was then cooled to 50 °C, and a mixture of azido-propylamine (0.53 g, 5.3 mmol, 1 equiv.) and pyridine (0.22 mL) was added dropwise. The mixture was left at 50 °C for 5 hours, then precipitated in acetone, filtered and lyophilized. The monofunctional DTPA (1) was purified by preparative HPLC separation (0.555 g, yield 30%). ¹H NMR (400 MHz, D₂O) δ ppm: 1.8 (2H, m, CH₂CH₂N₃), 3.4 (12H, t, N(CH₂)₂N and CH₂N₃), 3.7 (2H, s, NCH₂CO₂H), 4 (8H, s, NCH₂CO₂H). FT-IR (ATR, cm⁻¹): 2100 (N₃). LC-MS (ES⁺, *m/z*): 476.2 Da [M + H⁺].

2.3.3 Synthesis of Gd³⁺ complex (2). Pyridine (2 mmol, 0.16 mL) was added to azido-functionalized DTPA 1 (100 mg, 0.2 mmol) dissolved in few mL of H₂O and stirred for 10 minutes at

room temperature. $\text{GdCl}_3 \cdot 6\text{H}_2\text{O}$ (0.15 g, 0.4 mmol) was then added, and the mixture was left at 40 °C for 24 hours. Solvents were removed under vacuum, and an aqueous solution of the complex was stirred in Chelex resin 100 overnight to remove free Gd^{3+} .²³ The product was then filtered, lyophilized, and obtained as white solid. The absence of free gadolinium was verified by methyl thymol blue (MTB) calorimetric test²⁴ and the amount of complexed Gd^{3+} was calculated by ICP-MS, revealing 10% Gd by weight (64 mg; yield: 50%). MALDI-TOF (dithranol, m/z): $[\text{M} + \text{K}^+] = 685.8$ Da versus 685.78 calculated. FT-IR (ATR, cm^{-1}): 2100 (N_3).

2.3.4 Synthesis of propargyl methacrylate. Methacryloyl chloride (13.95 g, 133 mmol) in 50 mL DCM was added dropwise at 0 °C during 30 minutes to propargyl alcohol (5 g, 89 mmol) and Et_3N (13.51 g, 133 mmol) in 50 mL DCM. The reaction was then left overnight at room temperature. After removal of ammonium salts by filtration over celite, the product was washed with 3×50 mL of saturated NaHCO_3 and 3×50 mL H_2O until pH = 7. The product was dried over MgSO_4 and solvents were removed under reduced pressure. The final product was obtained as colorless oil by vacuum distillation. (4 g, yield = 36%) ^1H NMR (300 MHz, CDCl_3) δ (ppm): 1.97 (3H, s, $\text{CH}_3\text{-C}=\text{CH}_2$), 2.48 (1H, s, $\text{C}\equiv\text{CH}$), 4.76 (2H, s, OCH_2), 5.63 (1H, s, $\text{C}=\text{CHH}$), 6.18 (1H, s, $\text{C}=\text{CHH}$).

2.3.5 Synthesis of poly(methyl methacrylate-co-propargyl methacrylate). Polymerization was carried out in toluene solution using a standard Schlenk technique under inert atmosphere of argon. Typically, methyl methacrylate (5 g, 49.9 mmol, 97.5 equiv.) and propargyl methacrylate (0.158 g, 1.279 mmol, 2.5 equiv.), AIBN (0.05 g, 0.3 mmol, 1% w/w), and toluene (20 mL) were placed in an oven-dried Schlenk tube. The tube was fitted with a rubber septum. The solution was further degassed by three freeze-thaw-pump cycles. The resulting mixture was placed in a thermostatically controlled oil bath at 70 °C for 2 hours. The reaction was stopped with liquid nitrogen. The polymer (3) was precipitated in cold methanol, collected by filtration, and dried *in vacuo*. ^1H NMR (300 MHz, CDCl_3) δ (ppm): 3.5 (s, 3H, OCH_3) and 4.2 (s, 2H, $\text{CH}_2\text{-C}\equiv\text{CH}$). $M_{n,\text{SEC}} = 40\,000$ g mol^{-1} , $D = 1.8$.

2.3.6 Synthesis of MRI visible poly(methyl methacrylate). In a Schlenk tube were placed poly(methyl methacrylate-co-propargyl methacrylate) (50 mg, 2.2% mol propargyl unit), Gd DTPA complex (7 mg, 10 μmol , 1.2 equiv.), CuBr (1.5 mg, 10 μmol , 1.2 equiv.), and the least amount of DMF to solubilize the components. The tube was fitted with a rubber septum. The solution was further degassed by three freeze-pump-thaw cycles. The mixture was stirred under argon, and PMDETA (3.7 mg, 22 μmol , 2.4 equiv.) was added. The reaction was left at 40 °C for 48 hours. The crude material was purified by dialysis (dialyzing tubing 6000–8000 MWCO) against acetone which was renewed regularly. After 3 days, acetone was evaporated to yield pure gadolinated PMMA (4) (40 mg, yield 80%).

2.4. MRI visualization

2.4.1 Mesh preparation for MRI visualization. Meshes were sprayed with PMMA MRI contrast agent having different Gd^{3+}

percentages prepared as follows: the synthesized polymeric contrast agent has been diluted by commercial PMMA and dissolved in DCM to obtain 0.14, 0.23 and 0.79% w/w of Gd^{3+} . On commercial polypropylene mesh (3×3 cm^2) each polymeric solution was sprayed using Infinity Airbrush system supplied by Harder & Steenbeck (Osteinbeck, Germany) under a pressure of argon of 3 bars and at a distance of 5 cm. Meshes were dried overnight under vacuum to obtain a constant weight.

2.4.2 MR imaging protocol. MR imaging experiments were performed on a Bruker Biospec 70/20 system operating at a magnetic field of 7 T (Bruker, Wissembourg, France). The resonant circuit of the NMR probe was a 35 mm diameter birdcage resonator. Meshes (around 1 cm^2) were embedded in degassed 1% by weight agar gel prior to imaging. Gadolinium-free samples corresponded to a polypropylene mesh without Gd contrast agent. To test signal enhancement, T1 weighting was introduced into the MR images using an inversion pulse in rapid three-dimensional (3-D) acquisition with relaxation enhancement (RARE) sequence (TR = 3000 ms; mean echo time (T_{Em}) = 8 ms; RARE factor = 8; FOV = $3 \times 3 \times 1.5$ cm; matrix $128 \times 128 \times 64$). Inversion time was set at 1100 ms, sufficient to allow canceling of the embedding gel.

2.5. Stability and cytocompatibility studies

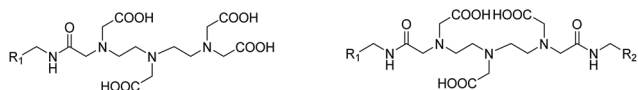
2.5.1 Film formation. Films containing different w/w% of Gd^{3+} have been prepared by diluting the MRI-visible polymer with commercial PMMA and dissolving in DCM. After solvent evaporation, films containing various amounts of Gd^{3+} were then obtained.

2.5.2 Stability studies. Films containing 0.10% and 0.43% by weight of Gd^{3+} were placed in PBS solution at 37 °C under stirring at 130 rpm. At scheduled time points (1, 7, 30 and 90 days) 1 mL of PBS buffer was withdrawn (then replaced by 1 mL fresh buffer) and analyzed by ICP-MS for Gd^{3+} release study.

2.5.3 In vitro cytotoxicity evaluation. Cytocompatibility tests were performed on L-929 murine fibroblast cells. Cells were cultured in MEM culture media by adding horse serum (10% by volume), penicillin streptomycin and 1% GLUTAMAX. Cells were grown in 5% CO_2 incubator at 37 °C for around 24 hours till a confluence of around 80%. At this point, the culture medium was sucked out and thrown. Different films were then gently placed on these cells. The films contained 0.23, 0.5 and 1.34% Gd^{3+} by weight. Films of gadolinium-free poly(methyl methacrylate-co-propargyl methacrylate) were also placed in addition to blank samples, negative control (the cells with cell lysis) and positive control (the cells). To each of the wells 1000 μL of LDH reaction mixture was added and samples were incubated for 24 hours. Each sample was repeated 3 times. After 24 hours, 10 μL of each sample were transferred to UV wells to which 100 μL of LDH were added. Sample was tested for UV absorbance at 490 nm by Victor V3 Perkin Elmer UV spectrophotometer.

3. Results and discussion

Azido mono-functionalized diethylenetriaminepentaacetic acid (compound 1) was synthesized in one step using DTPA



Scheme 2 Chemical structure of mono-amide DTPA and bis-amide-DTPA.

bis(anhydride) according to the procedure outlined in Scheme 1. In order to synthesize this DTPA ligand, a versatile method is the reaction of an amino precursor, namely the azidopropylamine, with DTPA bis(anhydride). However, the reaction of DTPA bisanhydride with amine groups usually yields a mixture of mono-amide and bis-amide products,^{25–27} and the separation can be difficult and fastidious depending on the type of amine used (Scheme 2).

Moreover, the synthesis of bis-amide-DTPA is relatively easy using an excess of amine without the need for tedious purification steps. Indeed, many publications reported the synthesis in which an excess of amine is used to ensure the formation of bis-amide.^{28,29} Perez-Baena *et al.* reported the synthesis of alkyne functionalized bis-amide DTPA in almost quantitative yield.³⁰ Azido-functionalized bis-amide DTPA ligands were also described.²⁰ Both ligands were used as MRI CAs and were grafted onto macromolecular architectures *via* click chemistry reactions. To the best of our knowledge, only few publications are reporting on mono-amide DTPA compounds. The main reason resides in the fact that these compounds are usually obtained in low yields with multi-step reactions. For example, a mono-maleimide derivative of DTPA bearing an amide link was prepared in a multi-steps reaction leading to a global low yield.³¹ Despite the challenging synthesis, mono-amide DTPA ligands are more interesting than bis-amide because the chelating power of DTPA in mono-amide DTPA is higher than in the corresponding bis-amide DTPA.²⁵ Another study revealed that micelles containing gadolinium monoamide DTPA complexes showed higher relaxivity than micelles with bis-amide DTPA complexes.³² In addition, the dissociation rate of linear bisamide Gd-DTPA chelates is higher than in other chelates due to insufficient thermodynamic and kinetic stabilities.³³ Moreover, compared to DOTA ligand, DTPA ligand has been chosen because the chemistry to prepare functional ligand is probably more simple, and DTPA is much cheaper than DOTA.

Therefore, the aim was to find a simple and versatile method to synthesize azido mono-functionalized DTPA ligand under mild conditions. DTPA ligand **1** was prepared in one step by condensation of the commercially available DTPA bis(anhydride) with azidopropylamine in DMF at 80 °C in the presence of imidazole. It was found that the optimal condition is an equimolar ratio between DTPA bis(anhydride) and azidopropylamine. Imidazole was used for its good promotion ability attributed to the low melting point of imidazolium salt, and its ability to homogenize the reaction mixture in dry media.³⁴ The LC-MS spectrum of the crude material revealed the presence of mono-functionalized DTPA and di-functionalized DTPA (Fig. S1†). After preparative HPLC separation, pure azido mono-

functionalized DTPA **1** was obtained as a white powder with a 30% yield. The LC-MS spectrum revealed the presence of a unique peak at 476.2 Da [$M + H^+$] as compared to 476.45 theoretical (Fig. S2†). The formation of the target compound was further confirmed by ¹H NMR (Fig. S3†) and FTIR. FT-IR analysis revealed the presence of the azide group at 2100 cm⁻¹.

The functionalized ligand **1** was then complexed with GdCl₃·6H₂O resulting in a gadolinium complex **2** with a quantitative yield. Purification on Chelex 100 resin was used to efficiently remove the free non complexed Gd³⁺. The absence of free Gd³⁺ was confirmed by a methyl thymol blue test (MTB) using UV spectroscopy. MALDI-TOF analysis using dithranol as a matrix revealed one peak at [$M + K^+$] = 685.8 Da as compared to 685.78 theoretical. The complexation ratio of Gd³⁺ in **1** was determined by ICP-MS and was found to be 40%. Further experiments were done in order to improve the complexation ratio. Unfortunately, the complexation ratio was not improved as it is not judicious to increase the temperature due to the thermo-labile azide groups. In fact, in most cases high temperature and long reaction time were used to increase the complexation ratio. Moreover, it is well-known that commercial DTPA CAs like Magnevist® contained non complexed ligands. Finally it is interesting to have an excess of ligand to reduce the proportion of the uncomplexed toxic free gadolinium.

MRI-visible poly(methyl methacrylate) (**4**) was obtained by combination of free radical polymerization and Huisgen click chemistry. First, poly(methyl methacrylate-*co*-propargyl methacrylate) with 2.5% of propargyl methacrylate monomer units was synthesized by free radical polymerization in toluene using AIBN as initiator and without any protection of the alkyne bond (Table 1). Best reaction conditions were found by using 1% by weight AIBN and a reaction time of 2 hours (entry 3). Experimental molar mass ($M_{n,exp} = 40\,000\text{ g mol}^{-1}$) determined by SEC was in good agreement with the expected value. Indeed, the molar mass of the PMMA polymer has to be high enough to allow a perfect coating of materials. Copolymers having 2.3% propargyl units were obtained as shown by ¹H NMR. Experimental molar ratios were in good agreement with theoretical compositions, which is consistent with a good incorporation of propargyl methacrylate monomer during the polymerization and a low loss of alkyne moiety. Nevertheless, protective groups such as trialkylsilyl can be used to overcome this problem. In our contribution, in order to limit the loss of alkyne group during the free radical polymerization, polymerizations were

Table 1 Characteristics of the poly(methyl methacrylate-*co*-propargyl methacrylate) copolymers

Entry	AIBN %wt	Time hours	Conv ^a %	$F_{PMA,exp}^a$	$M_{n,SEC}^b$ g mol ⁻¹	D^b
1	0.5	2	30	1.8	45 000	1.6
2	0.5	4	50	1.6	54 000	2
2	1	2	40	2.3	40 000	1.8
3	1	4	52	2.0	33 000	2

^a Determined by ¹H NMR. ^b Determined by size exclusion chromatography in THF.

Table 2 Characteristics of the macromolecular contrast agent

Gd content wt% calculated	Gd content ^a wt% experimental	Reaction efficiency (%)	Yield (%)
2.25	1.34	60	80

^a Determined by ICP-MS.

carried at 70 °C for a short time period, typically 2 hours, for the entry 3. As a consequence, conversion ratio of the polymerization remains low, below 50%.

To prepare MRI-visible poly(methyl methacrylate) polymer **4**, alkyne-functionalized PMMA **3** was coupled with azido mono-functionalized Gd-DTPA **2** by copper-catalyzed azide-alkyne cycloaddition (CuAAC). Click reaction was performed in DMF at 40 °C using a CuBr/PMDETA complex as catalyst. The reaction was stopped after 48 hours, and the macromolecular CA was then purified by dialysis against acetone using dialysis membranes with MWCO 6000–8000. The amount of Gd³⁺ in the polymeric CA was then measured by ICP-MS analysis as presented in Table 2. The calculated weight percentage of Gd³⁺ was 2.25, while the experimental weight percentage was 1.34. The difference between the calculated and the experimental values is due to the low efficiency of the click reaction, *i.e.* 60%. However, it is well-known that the efficiency of Huisgen click reaction is not quantitative in macromolecular chemistry due to the steric hindrance, the poor solubility of the reactant, *etc.* Nevertheless, the amount of Gd³⁺ into the macromolecular contrast agent is high enough for the next step, the coating of polypropylene mesh. ICP-MS measurements showed the copper amount in the macromolecular CA is below 1 ppm.

MRI-visible PMMA CA was then sprayed onto commercial polypropylene mesh using the airbrushing technique. The airbrushing is a versatile method allowing the preparation of homogenous and regular film without altering the mesh shape and mesh mechanical properties.¹⁹ Moreover, it was found that Gd-DTPA-PMMA using a PMMA with a molar mass of 40 000 g mol⁻¹ had suitable filmogenic properties on polypropylene mesh.

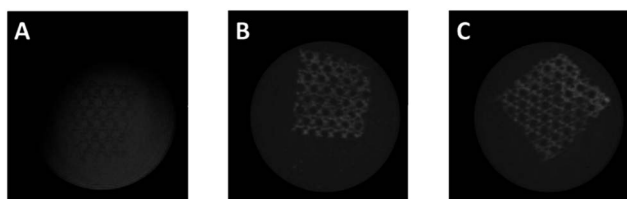
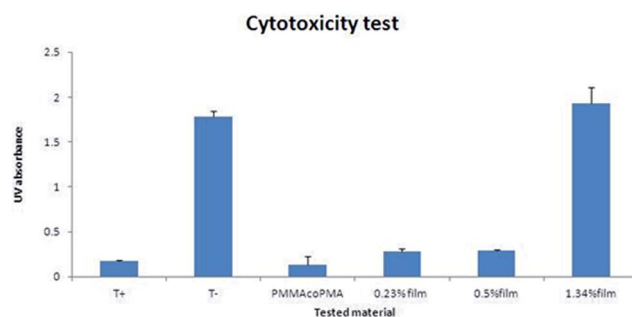
The effect of the proportion of Gd³⁺ in the polymeric CA on MRI visualization is shown on Fig. 1. Polypropylene meshes covered with CA were visualized using 7T MRI. In a first step, a 7T MRI scanner was used for preliminary studies. Then, further experiments will be done with a clinical scanner (1.5 T or

3 T). In the absence of CA, the polypropylene mesh was not visible. The mesh turned out to be visible by spraying it with the polymeric CA. For this, polypropylene meshes were coated with PMMA samples at different Gd³⁺ concentrations of 0.14 and 0.24% by weight. The amounts of Gd³⁺ present on each mesh were 1.4 and 2.3 µg per mg of polymeric contrast agent sprayed on the mesh. The amounts were determined depending on the amount of contrast agent placed on the mesh usually around 10 mg. Regardless the amount of Gd³⁺, meshes turned out to be visible even with concentrations of Gd³⁺ as low as 1.4 µg per mg of polymeric contrast agent, corresponding to 0.14% by weight Gd³⁺. The presence of 0.14% by weight of Gd³⁺ in the polymeric CA was sufficient to make the mesh visible. However, with the increase of Gd³⁺ content no signal enhancement or magnetic susceptibility effect were observed for MRI visualization.

Gd-complexes are gaining more importance because of nephrogenic systemic fibrosis (NSF). NSF mainly occurs in patients with severe renal failure. These patients take longer time to clear Gd-complexes, which increases the risk of transmetallation between Gd³⁺ and Zn²⁺ thus releasing free Gd³⁺.³⁵ For this, stable contrast agents are a necessity to eliminate any risks associated with free Gd³⁺ and prevent the precipitation of gadolinium salts.

In vitro stability studies were carried out in PBS buffer to detect any release of free toxic gadolinium and to evaluate long-term MR imaging. Circular films were prepared with the PMMA contrast agent containing 0.1 and 0.43% by weight of Gd³⁺ and placed in PBS buffer at 37 °C up to 90 days. The amount of released Gd³⁺ was measured by ICP-MS analysis. Films containing 0.1% Gd³⁺ w/w showed no detectable release of Gd³⁺ in PBS over a period of 90 days. Films containing 0.43% Gd³⁺ by weight (79 µg of Gd³⁺) showed a release of 0.4% Gd³⁺ (0.231 µg Gd³⁺) throughout the 90 days. In both cases this represents a very low release of Gd³⁺ showing the stability of the CA during this period of time. Moreover, µgram scale of gadolinium use can be compared to gram scale of gadolinium use for conventional MR scan where patients receive 1.0–2.5 g Gd³⁺ as a bolus (posology of 0.1–0.2 mmol kg⁻¹ of contrast agent for an intravenous injection of Magnevist).

MRI-PMMA CAs with different amounts of Gd³⁺ (0.23, 0.5, and 1.34% Gd³⁺) were placed in contact with murine fibroblast cells in order to determine their cytocompatibility. Fig. 2 showed that MRI-PMMA with 0.23 and 0.5% Gd³⁺ were cytocompatible and did not have any effect on cell growth after 24

**Fig. 1** 7T MR images of polypropylene meshes coated with polymeric contrast agents containing (A) blank (B) 0.14%, and (C) 0.23% by weight Gd³⁺.**Fig. 2** Effect of amount of Gd³⁺ present in film on UV absorbance.

hours whereas those containing 1.34% Gd³⁺ were detrimental for the cells. The LDH direct contact cytotoxicity test used to assess the cytocompatibility works as follows: LDH or lactate dehydrogenase is an enzyme liberated in culture media once cells are dead. The presence of LDH reduces tetrazolium salt in LDH mixture to formazan dye having a red color and a maximum absorbance at 490 nm. Thus, the presence of dead cells is indicated by both a red color and high UV absorbance at this wavelength. This had been the case with the TCPS negative control which contained the cell lysis, and in the case of the direct contact of PMMA MRI films containing 1.34% Gd³⁺ as revealed in Fig. 2. The graph also reveals that MRI PMMA films containing 0.23 and 0.5% Gd³⁺ (w/w) had almost no UV absorbance, and thus no cytotoxicity was observed. The result is not surprising because a study performed by Porsio *et al.*³⁶ revealed that MRI visible PCL nanoparticles with 1% Gd³⁺ (w/w) caused lower cell proliferation as compared to the same nanoparticles with lower Gd³⁺ amounts. Hence, polymeric contrast agents with the least amounts of Gd³⁺ are recommended in order to assure cytocompatibility by keeping a good MRI visibility.

4. Conclusion

This work described the synthesis of a new azido monofunctionalized DTPA ligand using a simple pathway for long term visualization of implanted meshes. The complexation of this DTPA ligand with Gd³⁺ lead to the synthesis of Gd-DTPA contrast agent. Macromolecular contrast agents based on poly(methyl methacrylate) were prepared by click chemistry of the Gd-DTPA ligand bearing an azide group onto alkyne-functionalized PMMA. This new MRI-visible polymer was characterized by ICP-MS analysis in order to determine the amount of gadolinium. The results revealed that an increase in the amount of Gd³⁺ did not improve visualization of the mesh. Thus amounts of Gd³⁺ as low as 0.1% by weight rendered polypropylene meshes visible on a 7T MRI. PMMA MRI contrast agents with amounts of Gd³⁺ as low as 0.1% by weight were also cytocompatible and stable. This allows their long-term use in the body for biomedical applications after further *in vivo* stability studies.

Acknowledgements

The authors thank the Balamand Internal Research Grant (BIRG) and the SATT AxLR for funding. The authors also thank Synbio3 platform (IBMM, Montpellier) for the preparative HPLC experiments and PRIMEx-IRM platform (Angers University) for the MRI resource.

Notes and references

- 1 R. Sutton, E. Kanal, B. Wilkoff, D. Bello, R. Luechinger, I. Jenniskens, M. Hull and T. Sommer, *Trials*, 2008, **9**, 68.
- 2 K. Jung, H. Kim, G. Lee, D. Kang, J. Park, K. Kim, Y. Chang and T. Kim, *J. Med. Chem.*, 2011, **54**, 5385–5394.
- 3 B. Nottelet, V. Darcos and J. Coudane, *Eur. J. Pharm. Biopharm.*, 2015, **97**, 350–370.

- 4 P. Caravan, J. Ellison, T. McMurry and R. Lauffer, *Chem. Rev.*, 1999, **99**, 2293–2352.
- 5 A. Sherry, P. Caravan and R. Lenkinski, *Chin. J. Magn. Reson. Imaging*, 2009, **30**, 1240–1248.
- 6 S. Aime and P. Caravan, *Chin. J. Magn. Reson. Imaging*, 2009, **30**, 1259–1267.
- 7 J. Bryson, J. Reineke and T. Reineke, *Macromolecules*, 2012, **45**, 8939–8952.
- 8 G. Schuhmann-Giampieri, H. Schmitt-Willich, T. Frenzel, W. Press and H. Weinmann, *Invest. Radiol.*, 1991, **26**, 969–974.
- 9 F. Fernández-Trillo, J. Pacheco-Torres, J. Correa, P. Ballesteros, P. Lopez-Larrubia, S. Cerdán, R. Riguera and E. Fernandez-Megia, *Biomacromolecules*, 2011, **12**, 2902–2907.
- 10 B. Doan, J. Seguin, M. Breton, R. Beherec, M. Bessodes, J. Rodríguez-Manzo, F. Banhart, J. Beloeil, D. Scherman and C. Richard, *Contrast Media Mol. Imaging*, 2012, **7**, 153–159.
- 11 R. Bolskar, *Nanomedicine*, 2008, **3**, 201–213.
- 12 C. Brown and J. Finch, *Ann. R. Coll. Surg. Engl.*, 2010, **92**, 272–278.
- 13 V. Letouzey, S. Huberlant, S. Blanquer, O. Guillaume, X. Garric and R. de Tayrac, *J. Minim. Invasive Gynecol.*, 2011, **18**, S117.
- 14 F. Franconi, J. Roux, X. Garric and L. Lemaire, *Magn. Reson. Med.*, 2014, **71**, 313–317.
- 15 N. Kraemer, J. Otto, M. Hostenius, I. Slabu, M. Baumann, U. Klinge, A. Muellen, B. Obolenski, R. Guenther and G. Krombach, *Proc. Intl. Soc. Mag. Reson. Med.*, 2009, 663.
- 16 N. Kuehnert, N. Kraemer, J. Otto, H. Donker, I. Slabu, M. Baumann, C. Kuhl and U. Klinge, *Surgical Endoscopy*, 2011, **26**, 1468–1475.
- 17 E. Schopf, J. Sankaranarayanan, M. Chan, R. Mattrey and A. Almutairi, *Mol. Pharm.*, 2012, **9**, 1911–1918.
- 18 S. Blanquer, O. Guillaume, V. Letouzey, L. Lemaire, F. Franconi, C. Paniagua, J. Coudane and X. Garric, *Acta Biomater.*, 2012, **8**, 1339–1347.
- 19 O. Guillaume, S. Blanquer, V. Letouzey, A. Cornille, S. Huberlant, L. Lemaire, F. Franconi, R. de Tayrac, J. Coudane and X. Garric, *Macromol. Biosci.*, 2012, **12**, 1364–1374.
- 20 S. El Habnoui, B. Nottelet, V. Darcos, B. Porsio, L. Lemaire, F. Franconi, X. Garric and J. Coudane, *Biomacromolecules*, 2013, **14**, 3626–3634.
- 21 A. Behrens, B. Casey, M. Sikorski, K. Wu, W. Tutak, A. Sandler and P. Kofinas, *ACS Macro Lett.*, 2014, **3**, 249–254.
- 22 B. Carboni, A. Benalil and M. Vaultier, *J. Org. Chem.*, 1993, **58**, 3736–3741.
- 23 P. Lebdušková, P. Hermann, L. Helm, É. Tóth, J. Kotek, K. Binnemans, J. Rudovský, I. Lukeš and A. Merbach, *Dalton Trans.*, 2007, 493–501.
- 24 J. Martinelli, B. Balali-Mood, R. Panizzo, M. Lythgoe, A. White, P. Ferretti, J. Steinke and R. Vilar, *Dalton Trans.*, 2010, **39**, 10056.
- 25 M. Ardestani, A. Arabzadeh, Z. Heidari, A. Hosseinzadeh, H. Ebrahimi, E. Hashemi, M. Mosayebnia, M. Shafiee-

- Alavidjeh, A. Alavi, M. Babaei, A. Rahmim, S. Ebrahimi and M. Amanlou, *J. Radioanal. Nucl. Chem.*, 2009, **283**, 447–455.
- 26 L. Frullano and P. Caravan, *Curr. Org. Synth.*, 2011, **8**, 535–565.
- 27 A. Vértes, *Handbook of nuclear chemistry*, Springer, Dordrecht, 2011.
- 28 P. Baía, J. André, C. Geraldes, J. Martins, A. Merbach and É. Tóth, *Eur. J. Inorg. Chem.*, 2005, **11**, 2110–2119.
- 29 T. Cheng, K. Lin, M. Ou, H. Shih, G. Liu and Y. Wang, *J. Chin. Chem. Soc.*, 2001, **48**, 1099–1105.
- 30 I. Perez-Baena, I. Loinaz, D. Padro, I. García, H. Grande and I. Odriozola, *J. Mater. Chem.*, 2010, **20**, 6916.
- 31 Y. Arano, T. Uezono, H. Akizawa, M. Ono, K. Wakisaka, M. Nakayama, H. Sakahara, J. Konishi and A. Yokoyama, *J. Med. Chem.*, 1996, **39**, 3451–3460.
- 32 T. Parac-Vogt, K. Kimpe, S. Laurent, C. Piérart, L. Elst, R. Muller and K. Binnemans, *Eur. J. Inorg. Chem.*, 2004, **17**, 3538–3543.
- 33 M. Ferreira, A. Martins, C. Martins, P. Ferreira, É. Tóth, T. Rodrigues, D. Calle, S. Cerdan, P. López-Larrubia, J. Martins and C. Geraldes, *Contrast Media Mol. Imaging*, 2013, **8**, 40–49.
- 34 A. Khalafinezhad, B. Mokhtari and M. Soltanirad, *Tetrahedron Lett.*, 2003, **44**, 7325–7328.
- 35 D. Broome, *Eur. J. Radiol.*, 2008, **66**, 230–234.
- 36 B. Porsio, L. Lemaire, S. El Habnoui, V. Darcos, F. Franconi, X. Garric, J. Coudane and B. Nottelet, *Polymer*, 2015, **56**, 135–140.